PCCP

Effects of Fixed Charge Group Physicochemistry on Anion Exchange Membrane Permselectivity and Ion Transport

Journal:	*Physical Chemistry Chemical Physics*
Manuscript ID	CP-ART-01-2020-000018.R1
Article Type:	Paper
Date Submitted by the Author:	27-Feb-2020
Complete List of Authors:	Ji, Yuanyuan; University of Virginia, Department of Chemical Engineering Luo, Hongxi; University of Virginia, Department of Chemical Engineering Geise, Geoffrey; University of Virginia, Department of Chemical Engineering

ARTICLE

Effects of Fixed Charge Group Physicochemistry on Anion Exchange Membrane Permselectivity and Ion Transport

Received 00th January 20xx,
Accepted 00th January 20xx

DOI: 10.1039/x0xx00000x

Yuanyuan Ji,[a] Hongxi Luo [a] and Geoffrey M. Geise *[a]

Understanding the effects of polymer chemistry on membrane ion transport properties is critical for enabling efforts to design advanced highly permselective ion exchange membranes for water purification and energy applications. Here, the effects of fixed charge group type on anion exchange membrane (AEM) apparent permselectivity and ion transport properties were investigated using two crosslinked AEMs. The two AEMs, containing a similar acrylonitrile, styrene and divinyl benzene-based polymer backbone, had either trimethyl ammonium or 1,4-dimethyl imidazolium fixed charge groups. Membrane deswelling, apparent permselectivity and ion transport properties of the two AEMs were characterized using aqueous solutions of lithium chloride, sodium chloride, ammonium chloride, sodium bromide and sodium nitrate. Apparent permselectivity measurements revealed a minor influence of the fixed charge group type on apparent permselectivity. Further analysis of membrane swelling and ion sorption, however, suggests that less hydrophilic fixed charge groups more effectively exclude co-ions compared to more hydrophilic fixed charge groups. Analysis of ion diffusion properties suggest that ion and fixed charge group enthalpy of hydration properties influence ion transport, likely through a counter-ion condensation, ion pairing or binding mechanism. Interactions between fixed charge groups and counter-ions may be stronger if the enthalpy of hydration properties of the ion and fixed charge group are similar, and suppressed counter-ion diffusion was observed in this situation. In general, the hydration properties of the fixed charge group may be important for understanding how fixed charge group chemistry influences ion transport properties in anion exchange membranes.

1. Introduction

Ion exchange membranes (IEMs) are often prepared using charged polymers, i.e., polymers having ionizable fixed charge groups incorporated into the polymer matrix.[1-4] Anion exchange membranes (AEMs) contain positively charged groups and preferentially transport anions (i.e., counter-ions) while excluding cations (i.e., co-ions). Cation exchange membranes (CEMs) contain negatively charged groups and preferentially transport cations (i.e., counter-ions) while excluding anions (i.e., co-ions).[2, 3] Due to their ability to selectively transport specific ions, IEMs are often used as selective separators in diverse water purification (e.g., electrodialysis (ED) and membrane capacitive deionization (MCDI)), energy generation (e.g., reverse electrodialysis (RED)) and energy storage (e.g., redox flow battery (RFB)) applications.[3-8] Emerging technologies and/or applications introduce separation challenges whereby IEMs may be exposed to aqueous electrolyte solutions containing a variety of ions that are different from the traditionally and widely-studied sodium and chloride ions. For example, ED or MCDI processes have been considered for deionization of increasingly contaminated water containing iron,[9] chromium,[10] copper,[11] cadmium,[12] fluoride,[13] nitrate,[5] perchlorate,[14] sulfate,[5] and barium[15] ions. To realize efficient water purification and energy production using membrane-based technologies, IEMs must maintain high apparent permselectivity properties upon exposure to the specific ions of interest.[5, 7]

Efforts have been made to engineer membrane apparent permselectivity for specific ions, and most of these efforts have focused on engineering IEM polymer chemistry using two broad approaches.[16, 17] The first approach includes membrane surface chemistry modifications,[16] such as enhancing the degree of crosslinking on the membrane surface or creating a dense and neutral surface layer,[18] creating oppositely charged surface layers,[19-23] or creating "layer-by-layer" structures.[23-25] Several of these approaches appear to be effective in enhancing membrane selectivity between ions of different size or valence.[18] For example, increasing the degree of crosslinking (or otherwise densifying) the membrane surface may result in increased ion selectivity via a mechanism that differentiates ions based, typically, on hydrated radii.[18] Alternatively, selectivity between ions of different valence can be achieved by creating oppositely charged surface layers or "layer-by-layer" structures to leverage different extents of electrostatic exclusion.[23]

The second approach includes fixed charge group chemistry modifications.[16] The most commonly used anionic fixed charge group in CEMs is the sulfonate group,[26] but other anionic groups, e.g., carboxylic acid, phosphonic acid, boric acid, and phenolic acid, have been studied.[18, 27, 28] For example, boric acid

[a] Department of Chemical Engineering, University of Virginia, 102 Engineers' Way, P.O. Box 400741, Charlottesville, VA 22904 USA

Electronic Supplementary Information (ESI) available: See DOI: 10.1039/x0xx00000x

groups, in contrast to sulfonic acid groups, did not remarkably enhance selectivity between alkaline earth metal cations and sodium ions.[28] Alternatively, CEMs with phosphoric acid groups appear to be more effective at separating like-valent cations than CEMs with sulfonic acid groups.[27] A larger library of cationic fixed charge groups can be used to prepare AEMs, e.g., quaternary ammonium, quaternary phosphonium, quinuclidinium-based quaternary ammonium, imidazolium, pyridinium, and pentamethyl guanidinium groups. The influence of cationic fixed charge groups on AEM properties has been investigated primarily for alkaline fuel cell applications, and less attention has been given to aqueous electro-membrane applications. Therefore, this study aims to understand the influence of cationic fixed charge group type on AEM performance for aqueous electro-membrane separations.

Here, we studied the influence of cationic fixed charge group type on AEM apparent permselectivity and ion transport properties. Two acrylonitrile, styrene and divinyl benzene-based, crosslinked AEMs containing similar polymer backbones but different cationic fixed charge groups (i.e., either trimethyl ammonium, TMA, or 1,4-dimethyl imidazolium, DMI) were synthesized and studied. Apparent permselectivity and counter- and co-ion transport properties were characterized using electrolytes containing different counter-ions (i.e., sodium chloride, sodium bromide and sodium nitrate) or different co-ions (i.e., lithium chloride, sodium chloride and ammonium chloride).

The transport property differences, arising from differences in the fixed charge group and differences in the electrolytes exposed to the membranes, were analyzed and hypothesized to correlate with the physicochemical properties of membrane fixed charge groups (i.e., bulkiness and hydrophilicity) and ions (i.e., size and hydrophilicity). This hypothesis was based on the observation that fixed charge group bulkiness and hydrophilicity lead to specific interactions between ions and fixed charge sites in colloid, surfactant and biological systems. Overall, results from this study quantify the influence of fixed charge group chemistry on the apparent permselectivity properties of AEMs and provided insight into how fixed charge group chemistry influences ion transport.

2. Materials and Methods

2.1. Polymers

2.1.1. Structure

The polymer backbone of the two AEMs considered in this study was composed of styrene, acrylonitrile, divinyl benzene and styrene-based monomers (Figure 1). The composition of these monomers was controlled to be equivalent during the synthesis processes (described in Section 2.1.2). As such, the only expected significant difference between the two AEMs is the fixed charge group type. The two AEMs were named "PVBAN-TMA[X]" and "PVBAN-DMI[X]" (where "PVBAN" reflects the styrene (poly(vinyl benzene)) and acrylonitrile content of the material) and "TMA" or "DMI" specifies the fixed charge group: trimethyl ammonium (TMA) or 1,4-dimethyl imidazolium (DMI). The nomenclature "[X]" indicates that the membrane is in the X counter-ion form.

2.1.2. Synthesis

Unless otherwise noted, reagents/monomers were obtained from Sigma-Aldrich. Styrene (catalog number S4972), acrylonitrile (catalog number 110213), (vinylbenzyl)trimethylammonium chloride (catalog number 458694) and 1,2-dimethyl-3-(4-vinylbenzyl)imidazolium chloride were used as monomers. Divinylbenzene (catalog number 414565) was used as the crosslinker, and benzoin ethyl ether (catalog number 172006) was used as the photoinitiator.[29] Synthesis of 1,2-dimethyl-3-(4-vinylbenzyl)imidazolium chloride is described in Section S1 of the Supplementary Information. Inhibitors were removed from the vinyl monomers by using a *tert*-butylcatechol inhibitor remover (catalog number 311340).

The two AEMs were prepared via a photo-initiated crosslinking process.[30, 31] The reagent mixture used to prepare PVBAN-TMA[Cl] contained 0.20g styrene, 0.60g acrylonitrile, 0.24g (vinylbenzyl)trimethylammonium chloride, 0.041g divinyl benzene and 0.04g benzoin ethyl ether. The reagent mixture used to prepare PVBAN-DMI[Cl] contained 0.20g styrene, 0.60g acrylonitrile, 0.29g 1,2-dimethyl-3-(4-vinylbenzyl)imidazolium chloride, 0.044g divinyl benzene and 0.04g benzoin ethyl ether. As such, for both AEMs, the composition (by mass) of styrene and acrylonitrile, (vinylbenzyl)trimethyl ammonium chloride or 1,2-dimethyl-3-(4-vinylbenzyl)imidazolium chloride, divinyl benzene, and benzoin ethyl ether was approximately 70%, 24%, 4% and 2%, respectively.

To obtain a transparent homogeneous solution, 1g (total monomer) was mixed and ultrasonicated with 1.6g (dimethyl sulfoxide (DMSO)). Then, this solution was confined between two quartz plates to form a liquid film, and spacers were used to control the separation of the plates and, ultimately, the membrane thickness,[32] The solution was

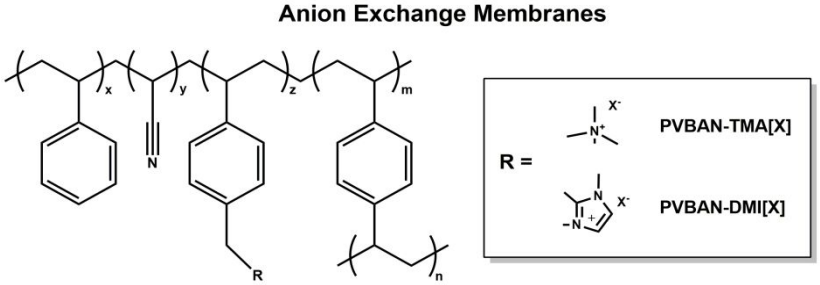

Figure 1. Polymer structure and nomenclature for the two anion exchange membranes (AEMs) considered in this study.

cured by irradiation with 120 μJ/cm^2 of 254 nm UV light for 1 hour to produce transparent polymer films that had a slight brown color.[29]

After curing, the membranes were carefully peeled from the glass plates and placed into Teflon dishes. The membranes were then dried at 60°C for 1 hour in a convection oven. This initial drying step did not completely remove DMSO from the sample, but it was a necessary step to prepare membranes that had sufficient mechanical strength to facilitate handling/study. Next, the membranes (still in the Teflon dishes) were dried under vacuum at 60°C for 48 hours. The mass of the membrane sample was measured both before and after the two drying steps, and we estimated that over 98% of the DMSO was removed from the membrane during this drying process.

Finally, the membrane was soaked in de-ionized (DI) water to fully hydrate the polymer and likely extract any unreacted hydrophilic monomers and/or residual DMSO. To minimize exposure to atmospheric carbon dioxide, which can affect AEMs via ion exchange,[33] membranes were quickly placed into a container completely filled with DI water obtained directly from the DI water system. The container was then immediately sealed to minimize exposure to atmospheric carbon dioxide.

2.1.3. Physicochemical Properties

Two fixed charge group physicochemical properties were considered: fixed charge group bulkiness and hydrophilicity. The fixed charge group bulkiness was quantified using the van der Waals volume (V_{vdw}),[34, 35] and the hydrophilicity was quantified using the enthalpy of hydration (ΔH_{hyd}).[36-38] The van der Waals volumes of the fixed charge groups were estimated using a semi-empirical group contribution method that relates the chemical structure/atomic makeup of an organic compound to its van der Waals volume.[34] The enthalpy of hydration values were estimated using a semi-empirical method that relates the charge density of an organic cation to its enthalpy of hydration.[37] The estimation processes are described in more detail in Section S2 of the Supplementary Information, and the results are presented in Table 1.

2.2. Methods

2.2.1. Dry Polymer Density

Dry polymer density (ρ_p) was measured using an Archimedes' principle method.[32] A Mettler Toledo density kit (Part #111067060, Mettler Toledo) was used in conjunction with an analytical balance (XSE204, Mettler Toledo). The mass of the dry polymer sample first was measured in air (m_1) and subsequently was measured in an auxiliary liquid, i.e., a non-solvent for the polymer (m_2). The dry polymer density was calculated as:

$$\rho_p = \frac{m_1}{m_1 - m_2}(\rho_2 - \rho_1) + \rho_1 \quad (2)$$

where ρ_1 and ρ_2 are the density values, at the measurement temperature, of air and the auxiliary liquid, respectively. *N*-heptane was used as the auxiliary liquid for both AEMs because *n*-heptane sorption in polyacrylonitrile was negligible, and the molar composition of acrylonitrile in the AEMs was over 85%. The measurement temperature (i.e., the air and auxiliary liquid temperatures) was recorded for each measurement, and the density values for air and *n*-heptane were evaluated at the measurement temperature.[39]

2.2.2. Water Uptake

Water uptake (w_u) was measured using samples that had been equilibrated with either DI water or 0.5mol/L aqueous electrolyte solutions. Prior to the measurement, smaller circular sample coupons were cut from larger membrane films. These coupons had diameters of 0.95cm or 1.27cm. To measure water uptake in DI water, the samples were placed in a container that was then completely filled with DI water obtained directly from the DI water system. The container was sealed immediately after filling to minimize exposure to atmospheric carbon dioxide. This was done to minimize ion exchange from the chloride to carbonate or bicarbonate counter-ion form.[33] The samples were allowed to equilibrate in DI water for at least 48 hours before continuing with the procedure.

To measure water uptake in 0.5mol/L aqueous electrolyte solutions of lithium chloride, sodium chloride or ammonium chloride, the circular coupon samples were allowed to equilibrate in the electrolyte solution for at least 48 hours. To measure the water uptake in 0.5mol/L solutions of sodium bromide and sodium nitrate, the samples were allowed to equilibrate in the electrolyte solution for at least 72 hours, and fresh solution was used to replace the old solution every 12 hours. The solution replacement procedure was used to ensure complete counter-ion exchange with the solution.

Following the initial equilibration in either DI water or electrolyte solution, the samples were removed from the DI water or electrolyte solution, and the wet mass (m_{wet}) was measured (XSE204, Mettler Toledo) quickly after the excess DI water or electrolyte solution was removed from the sample surface using a laboratory wipe. The sample subsequently was dried under vacuum at ambient temperature until a stabilized dry mass (m_{dry}) was obtained. The drying process typically required 36 to 48 hours. The dry mass was measured immediately after the drying process to prevent sorption of

Table 1. Estimated van der Waals volume and enthalpy of hydration values for the two fixed charge groups considered in this study. The values were calculated using semi-empirical models adapted from the literature and described in more detail in Section S2 of the Supplementary Information.

Membrane and Fixed Charge Group		Estimated Van der Waals Volume, V_{vdw} [Å^3]	Estimated Enthalpy of Hydration, ΔH_{hyd} [kJ/mol]
PVBAN-TMA[X]	Trimethyl ammonium	72	-272
PVBAN-DMI[X]	1,4-Dimethyl imidazolium	99	-260

moisture from the atmosphere. The water uptake (w_u) was calculated as:

$$w_u = \frac{m_{wet} - m_{dry}}{m_{dry}} \quad (3)$$

The water uptake for each membrane was reported as the average of at least five measurements, and the uncertainty was taken as one standard deviation from the mean. The volume fraction of water (ϕ_w) in the membrane was calculated using the measured dry polymer density and water uptake data via a volume additivity approach:[40]

$$\phi_w = \frac{w_u/\rho_w}{w_u/\rho_w + (1-w_u)/\rho_p} \quad (4)$$

where ρ_w is the density of water, which was taken as 1g/cm^3.[39]

2.2.3. Ion Exchange Capacity and Fixed Charge Concentration

The membrane ion exchange capacity (*IEC*) represents the concentration of fixed charge groups in a dry polymer membrane and has the unit of [milliequivalents (fixed charge groups) / g (dry polymer)]. Here the *IEC* was determined using an ion exchange method. This method recognizes that the ion exchange process is described by counter-ion specific equilibrium constants.[41] For example, in strong-base ion exchangers (such as those considered here), the nitrate counter-ion has a greater ion exchange equilibrium constant than the chloride counter-ion.[41] Therefore, when a chloride counter-ion form AEM is exposed to a nitrate-containing solution, nitrate will preferentially replace the chloride counter-ions in the AEM via ion exchange. Thus, the *IEC* can be determined by measuring the amount of chloride released by an initially chloride counter-ion form membrane upon exposure to a sufficiently high volume and concentration aqueous sodium nitrate solution, which will promote ion exchange to the nitrate counter-ion form.

Prior to the *IEC* measurement, chloride counter-ion form membranes were cut into circular coupons with diameters of either 0.95cm or 1.27cm. The coupons were then soaked in a volume v_E of 1mol/L $NaNO_3$ solution (v_E was either 50mL for the 0.95cm diameter samples or 80mL for the 1.27cm diameter samples). After ion exchange was complete, the chloride concentration of the resulting external solution (c_E) was measured using ion chromatography (ICS-2100, Thermo Scientific). Finally, the coupons were soaked in DI water to allow excess sodium nitrate to desorb from the sample and subsequently dried under vacuum. The dry mass (m_{dry}) was measured, and the *IEC* was calculated as:

$$IEC = \frac{v_E c_E}{m_{dry}} \quad (5)$$

The fixed charge group concentration (c_A^m) is the concentration of fixed charge groups in the water sorbed by the membrane and has the unit of [milliequivalents (fixed charge groups) / cm^3(water sorbed)]. The value of c_A^m was calculated as:

$$c_A^m = \frac{IEC}{w_u}\rho_w \quad (6)$$

2.2.4. Apparent Permselectivity

Apparent permselectivity (α) was measured using a static method.[42, 43] The membrane potential (E_m) was measured using Ag/AgCl double junction electrodes (RREF 0024, Pine Instrument Co.) while the sample separated 100mL solutions of high ($a_\pm^{sL}$) and low ($a_\pm^{s0}$) mean ionic activity (i.e., high and low concentration electrolyte solutions), and the apparent permselectivity was calculated as:

$$\alpha = \frac{\left[E_m \Big/ \left(\frac{RT}{F} \ln \frac{a_\pm^{sL}}{a_\pm^{s0}} \right) + 1 - 2t_M^s \right]}{2t_X^s} \quad (7)$$

where R is the gas constant and F is Faraday's constant. The apparent permselectivity of each sample was measured three times, and the uncertainty was taken as one standard deviation from the mean.

The measurement temperature was maintained at 23±2°C, and apparent permselectivity is not expected to vary significantly over this temperature range.[42] The counter-ion and co-ion transport numbers in the solution phase were calculated using diffusion coefficients in aqueous solution at infinite dilution and 25°C.[44] The low (c_0) and high (c_L) solution concentrations were chosen to be 0.1mol/L and 0.5mol/L to be consistent with other studies. The mean ionic activity values were determined as:

$$a_\pm^{s0} = \gamma_\pm^{s0} c_0 \quad (8)$$

$$a_\pm^{sL} = \gamma_\pm^{sL} c_L \quad (9)$$

where $\gamma_\pm^{s0}$ and $\gamma_\pm^{sL}$ are the average electrolyte activity coefficients on the low and high concentration side of the membrane, respectively and were determined using the Pitzer model.[45] Samples of apparent permselectivity calculations are provided in Section S3 of the Supplementary Information.

The electrode filling solution was 1mol/L potassium nitrate solution, and the electrodes were used to measure electrical potential in 0.1mol/L and 0.5mol/L aqueous solutions of either lithium chloride, sodium chloride, ammonium chloride, sodium nitrate or sodium bromide. Junction potentials may occur between the reference electrode tip and the solution and could bias the apparent permselectivity measurement.[46] A reported junction potential correction was applied to the data, and the junction potential-corrected apparent permselectivity values are presented and discussed in Section S4 of the Supplementary Information. While the junction potential correction affected the magnitude of the apparent permselectivity, the qualitative trends in the data did not change as a result of applying the junction potential correction.

2.2.5. Ionic Conductivity

The membrane ionic conductivity (σ_m^s) was measured using electrochemical impedance spectroscopy (EIS, SP 150, Biologic). Prior to the measurement, samples were equilibrated with 0.5mol/L aqueous electrolyte solution. The measurement was

performed while the membrane separated two reservoirs that were filled with 50mL of 0.5mol/L aqueous solutions of either lithium chloride, sodium chloride, ammonium chloride, sodium nitrate or sodium bromide. The cross-sectional membrane area in the cell was 4.52cm^2. Platinum mesh electrodes that spanned the cross-sectional area of the cell were fixed on both ends of the cell, and Ag/AgCl reference electrodes (MF-2052, Bioanalytical Systems Inc., Lafayette, IN) were placed on either side of the membrane. The position of the reference electrodes was fixed during the entire measurement. The impedance response was measured from 1Hz to 50kHz with a current amplitude of 1mA. A total of 100 data points were recorded.

The ohmic resistance of the cell containing the solution and the membrane (R_{m+s}) was taken as the value of the real impedance when the imaginary impedance was zero (i.e., when the data on a Nyquist plot crossed the real axis). The cell was then disassembled, and the hydrated thickness of the membrane (δ) was measured (Model #293-244, Mitutoyo) immediately after the resistance measurement. The cell was then reassembled without the membrane, and the same measurement was repeated to obtain the resistance of aqueous solution (R_s). The conductivity of the membrane (σ_m^s) was calculated as:

$$\sigma_m^s = \frac{\delta}{A(R_{m+s} - R_s)} \tag{10}$$

where A is the cross-sectional area of the cell.

2.2.6. Salt Sorption and Diffusion Coefficients

The membrane salt sorption and diffusion coefficients were measured using a kinetic desorption technique.[43] To minimize the effects of carbon dioxide on the AEMs,[33] the entire process was performed under a nitrogen blanket. A container filled with 25mL DI water was sealed and purged with nitrogen until the conductivity decreased to and stabilized at approximately 0.10μS/cm. Electrolyte solution-equilibrated membrane coupons were removed from the solution, and the excess solution on the sample surface was quickly removed using a laboratory wipe. Then, the sample was quickly added to the container containing the nitrogen purged DI water, and the container was immediately re-sealed.

The conductivity of the desorption solution was recorded as a function of time using a conductivity meter (inoLab* Cond7310, WTW Corp Inc.). Since the entire apparatus was purged with nitrogen during the desorption process, it was necessary to correct for evaporative water loss. This water loss caused a consistent background increase in the solution conductivity throughout the experiment. To account for this background conductivity increase, background conductivity curves were determined for all of the electrolyte solutions considered. The detailed steps taken to obtain the background curves are discussed further in Section S5 of the Supplementary Information.

The "evaporation-corrected" desorption conductivity curve was obtained by subtracting the background conductivity curve from the measured desorption conductivity curve. Then, the conductivity was converted to salt concentration using a calibration curve. A flat-sheet diffusion model was used to determine the salt diffusion coefficient (D_s^m) in the membrane from the desorption data:[47]

$$D_s^m = \left\{ \frac{\pi\delta^2}{16} \left[\frac{\partial(M_t/M_\infty)}{\partial t^{\frac{1}{2}}} \right]^2 \right\} t^{\frac{1}{2}} \tag{11}$$

where M_t is the mass of salt desorbed from the polymer at time t, and M_∞ is the total mass of salt desorbed from the polymer during the entire experiment. Equation 10 is an approximation that is only valid when $M_t/M_\infty \leq 0.6$. Thus, the early-time desorption data were plotted as M_t/M_∞ versus $t^{1/2}$, and the term in square brackets was evaluated as the slope of that plot.

The salt sorption coefficient (k_s^m) was calculated as:

$$k_s^m = \frac{c_s^m}{c_s^s} = \frac{c_\infty^s v_d}{c_s^s v_p \phi_w} \tag{12}$$

where v_d is the desorption solution volume (set at the beginning of the experiment), and v_p is the hydrated sample volume. The sample volume was determined geometrically using the measured hydrated thickness (δ) and the diameter (d) of the circular coupon samples and $v_p = \pi d^2\delta/4$. The hydrated membrane thickness was measured using a micrometer (Model #293-244, Mitutoyo), and the thickness was measured at three different locations on the sample and averaged. The measurement was repeated three to four times for each sample with each electrolyte, and the salt sorption and diffusion coefficients were reported as the average and standard deviation of the data. More information regarding the analysis of the kinetic desorption is provided in Section S5 of the Supplementary Information.

3. Results and Discussions

3.1. Membrane Properties

The PVBAN-TMA and PVBAN-DMI polymers used in this study are considered to be dense non-porous membranes where transport through the material can be described via a solution-diffusion mechanism.[4, 17, 48, 49] Ions, due to their small size relative to the

Table 2. Hydrated thickness (δ), dry polymer density (ρ_p), ion exchange capacity (IEC) and water uptake (w_u) properties measured using DI water and the two chloride counter-ion form AEMs. Samples were equilibrated, prior to characterization, in DI water for at least 48 hours.

Polymer	δ [mm]	ρ_p [g / cm^3]	IEC [meq / g(dry polymer)]	w_u [g(water) / g(dry polymer)]
PVBAN-TMA[Cl]	0.060±0.01	1.22±0.03	1.2±0.2	0.61±0.03
PVBAN-DMI[Cl]	0.045±0.003	1.16±0.02	1.2±0.1	0.51±0.04

polymer network mesh, transport through such materials via free volume.[17, 50] The materials also contain the same base polymer backbone, suggesting that the polymer structure (e.g., mesh size) is likely very similar for the two polymers.

Membrane properties, measured in DI water, are reported in Table 2. The membrane composition was controlled to yield materials that had statistically equivalent ion exchange capacity (*IEC*) values. The membrane prepared using the more hydrophilic (i.e., more negative enthalpy of hydration) TMA fixed charge group sorbed about 17% more water compared to the membrane prepared using the less hydrophilic DMI fixed charge group. Thus, membrane water uptake was consistent with the hydrophilicity of the fixed charge group used on the polymer backbone.

Membrane water uptake, water volume fraction and fixed charge group concentration data for materials measured using 0.5mol/L aqueous electrolyte solutions are reported in Table 3. Generally, the water uptake of both membranes in 0.5mol/L aqueous electrolyte solutions decreased by 20 to 55% relative to that in DI water. This result is due, at least in part, to osmotic deswelling, as the thermodynamic activity of water exposed to the polymer is reduced by the presence of salt in the electrolyte solution.[17, 51] Additionally, the materials soaked in the bromide or nitrate containing

Table 3. Water uptake (w_u), water volume fraction (ϕ_w), and fixed charge group concentration (c_A^m) properties determined using samples that had been equilibrated in 0.5mol/L aqueous electrolyte solutions. Prior to characterization, samples were equilibrated in 0.5mol/L aqueous electrolyte solution for 48 to 72 hours. The sodium bromide and sodium nitrate solutions were replaced with fresh solution every 12 hours during equilibration to facilitate ion exchange from the initial chloride counter-ion form to the bromide or nitrate counter-ion forms, respectively. The water uptake and fixed charge concentration units are [g(water)/g(dry polymer)] and [meq/cm^3(sorbed water)], respectively.

Electrolytes	PVBAN-TMA[X]			PVBAN-DMI[X]		
	w_u	ϕ_w	c_A^m	w_u	ϕ_w	c_A^m
LiCl	0.47±0.02	0.36±0.01	2.6±0.3	0.30±0.01	0.26±0.01	3.8±0.4
NaCl	0.46±0.01	0.36±0.01	2.7±0.3	0.30±0.01	0.26±0.01	3.8±0.4
NH_4Cl	0.44±0.01	0.35±0.01	2.7±0.4	0.29±0.01	0.25±0.01	4.0±0.4
NaBr	0.38±0.02	0.32±0.02	3.2±0.4	0.26±0.02	0.23±0.02	4.4±0.6
$NaNO_3$	0.36±0.01	0.31±0.01	3.3±0.4	0.22±0.07	0.20±0.05	5.3±1.8

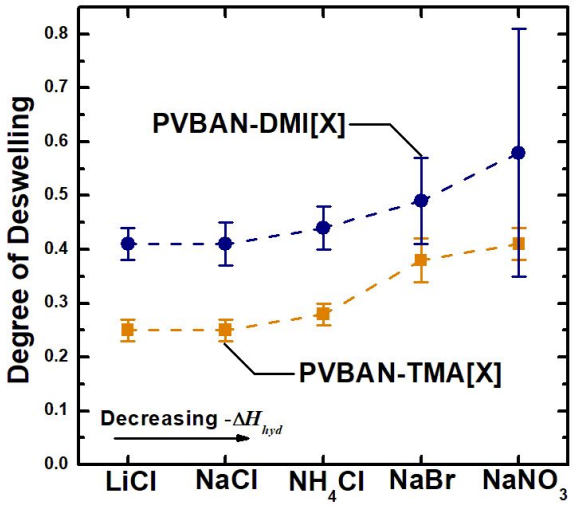

Figure 2. The degree of deswelling of the two AEMs measured using 0.5mol/L aqueous solutions of different electrolytes. The degree of deswelling is defined as [w_u (DI water) – w_u (electrolyte solution)] / [w_u (DI water)]. The $-\Delta H_{hyd}$ order of co-ions, counter-ions (Table 4) and fixed charge groups are: Cl^- > Br^- > NO_3^-, Li^+ > Na^+ > NH_4^+, trimethyl ammonium > 1,4-dimethyl imidazolium, respectively.

Table 4. Enthalpy of hydration properties of the counter-ions and co-ions considered in this study.

Ion	Enthalpy of hydration, ΔH_{hyd} [kJ/mol]
Li^+	–519
Na^+	–409
NH_4^+	–307
Cl^-	–381
Br^-	–347
NO_3^-	–314

electrolytes were ion exchanged into the bromide and nitrate counter-ion forms, respectively. This ion exchange process from the initial chloride counter-ion form may also influence water uptake.

It is useful, however, to consider the degree of deswelling, which is defined as the difference in the water uptake values measured in DI water and electrolyte solution normalized by the water uptake measured in DI water. This degree of deswelling, i.e., [w_u (DI water) – w_u (electrolyte solution)] / [w_u (DI water)], appears to correlate with the hydrophilicity of the fixed charge group, co-ion and counter-ion (Figure 2). First, the membrane with the less hydrophilic fixed charge group (i.e., DMI) generally deswelled 15% more than the membrane with the more hydrophilic fixed charge group (i.e., TMA). Second, membrane deswelling increased as the counter-ions or co-ions became less hydrophilic (Table 4). For example, both membranes deswell 3% more in ammonium chloride compared to the situation in sodium chloride, which is consistent with the observation that the ammonium co-ion is less hydrophilic than sodium (Table 4). Moreover, both membranes deswell 16% more in sodium nitrate than in sodium chloride, and the nitrate counter-ion is less hydrophilic than chloride (Table 4). The influence of counter-ion hydrophilicity on deswelling was generally found to be more pronounced than the influence of the co-ion hydrophilicity. This result is reasonable given that ion exchange membranes generally contain far more counter-ions compared to co-ions,[17, 51] so changes in counter-ion hydrophilicity would be more likely to affect the water content of the polymer than changes in co-ion hydrophilicity.[52, 53]

3.2. Apparent Permselectivity

Apparent permselectivity was measured to determine how the fixed charge group, counter-ion type, and co-ion type affect apparent permselectivity properties (Figure 3). Generally speaking, the fixed charge group and counter-ion type influenced the apparent permselectivity to a smaller extent than the co-ion type. This section discusses the nature and relative magnitudes of observed specific ion effects in the polymers.

Switching between the TMA and DMI fixed charge group did not appreciably affect the apparent permselectivity of most of the materials and/or electrolytes considered. The membranes characterized using ammonium chloride were an exception. The PVBAN-DMI[Cl] material had 6% greater apparent permselectivity compared to the PVBAN-TMA[Cl] material.

This observation opposes the general view that ion exchange materials with either higher fixed charge concentration or lower water uptake tend to be more selective compared to materials that have lower fixed charge concentration or higher water uptake.[17, 51] The higher fixed charge concentration in the DMI-containing materials does not translate into a higher apparent permselectivity. A potential explanation for this observation is that the less hydrophilic nature of the DMI fixed charge group compared to the TMA fixed charge group promotes counter-ion condensation or binding/pairing of the counter-ion with the fixed charge group. This phenomenon would reduce the effective fixed charge concentration of the material, and as such, it could explain why the apparent permselectivity does not appreciably increase upon switching from the TMA to DMI fixed charge group as suggested by the combination Donnan theory[17, 51] and the water uptake, density and IEC measurements used to determine the fixed charge concentration.

Ion exchange of the material from the initial chloride counter-ion form to the bromide counter-ion form did not affect the apparent permselectivity when solutions containing the corresponding counter-ion were used to perform the characterization. Alternatively, the apparent permselectivity decreased when the nitrate counter-ion was used to characterize the apparent permselectivity properties of the nitrate counter-ion form materials. This result may be explained by interactions between the counter-ion and the fixed charge group, as will be discussed subsequently.

Changing the co-ion that was used to characterize the materials had a greater influence on the apparent permselectivity properties compared to the influence of fixed charge group or counter-ion type.

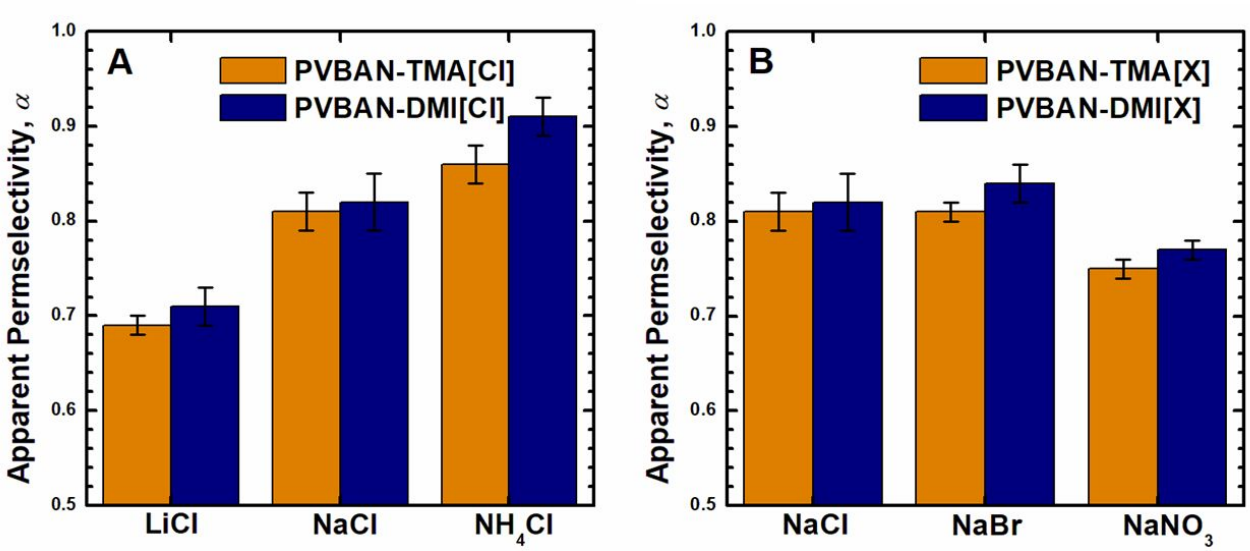

Figure 3. Membrane apparent permselectivity of the TMA- and DMI-containing AEMs measured using 0.1mol/L and 0.5mol/L aqueous electrolyte solutions of (A) lithium chloride, sodium chloride and ammonium chloride (i.e., electrolytes containing different co-ions) and (B) sodium chloride, sodium bromide and sodium nitrate (i.e., electrolytes containing different counter-ions).

The apparent permselectivity was greatest when ammonium was used as the co-ion and smallest when lithium was used as the co-ion (Table 3A). The observation that the ammonium chloride apparent permselectivity was higher than the sodium chloride apparent permselectivity is consistent with measurements made on commercially available AEMs.[54] The change in apparent permselectivity that was observed as the co-ion used in the measurement was changed correlates with the enthalpy of hydration of the co-ions in that the most hydrophilic co-ion (i.e., lithium) had the lowest apparent permselectivity, and the highest apparent permselectivity was measured using the least hydrophilic co-ion (i.e., ammonium).

3.3. Ion Transport Analysis: Sorption and Diffusion Ratios

To further explore the influence of ion type on apparent permselectivity, it is useful to consider an expression for the permselectivity that derives from the transport numbers of the counter-ion and co-ion in the membrane and solution phases, respectively.[54] The ion transport numbers in the membrane or solution phases are defined by the ion valence, concentration and diffusivity in the respective phases and represent the fraction of current carried by the ion under an applied electric field.[48] Three ratios can be used to describe the thermodynamic sorption and diffusion contributions to the apparent permselectivity:

$$\alpha = 1 - \frac{k^m_{X/M} D^m_{X/M} (1 + \frac{1}{D^m_{X/M}})}{k^m_{X/M} D^m_{X/M} + 1} \quad (13)$$

where the thermodynamic sorption ratio ($k^m_{X/M}$) is defined as the co-ion concentration in the membrane divided by the counter-ion concentration in the membrane, i.e., $k^m_{X/M} = c^m_X / c^m_M$. The membrane-phase diffusivity ratio ($D^m_{X/M}$) is defined as the co-ion diffusion coefficient in the membrane phase divided by the counter-ion diffusion coefficient in the membrane phase, i.e., $D^m_{X/M} = D^m_X / D^m_M$. The solution-phase diffusivity ratio ($D^s_{X/M}$) is defined as the co-ion diffusion coefficient in solution divided by the counter-ion diffusion coefficient in solution, i.e., $D^s_{X/M} = D^s_X / D^s_M$.

The value of $k^m_{X/M}$ quantifies the extent of co-ion relative to counter-ion sorption in the membrane phase, and $D^m_{X/M}$ quantifies the relative rates of co-ion and counter-ion diffusion within the membrane. Larger $k^m_{X/M}$ and $D^m_{X/M}$ values suggest a greater extent of co-ion transport compared to counter-ion transport in the membrane, and this situation would be expected to lead to a smaller permselectivity. The value of $D^s_{X/M}$ quantifies the relative rates of co-ion and counter-ion diffusion in solution, and this ratio captures ion specific diffusion in solution.

The $k^m_{X/M}$, $D^m_{X/M}$ and $D^s_{X/M}$ values influence permselectivity to different extents, and the influence of $k^m_{X/M}$ is the most pronounced (Section S6 of the Supplementary Information), which is not surprising as ion exchange membrane permselectivity properties are expected to result from Donnan exclusion of co-ions.[17, 51] For example, a 20% increase in $k^m_{X/M}$, $D^m_{X/M}$ and $D^s_{X/M}$ is expected to cause a 6% decrease, 2% decrease and 3% increase in permselectivity, respectively. As such, the co-ion sorption properties are important for understanding ion specific permselectivity properties.

To further analyze the measured apparent permselectivity properties (Figure 3), values of $k^m_{X/M}$, $D^m_{X/M}$ and $D^s_{X/M}$ were determined for the AEMs. Measurements of k^m_s , c^m_A , D^m_s and σ^m_s can be combined with parameter definitions and the Nernst-Einstein equation[55] to calculate the three ratios:

$$k^m_{X/M} = \frac{c^m_X}{c^m_M} \quad (14)$$

$$c^m_X = c^s_s k^m_s \quad (15)$$

$$c^m_M = c^s_s k^m_s + c^m_A \quad (16)$$

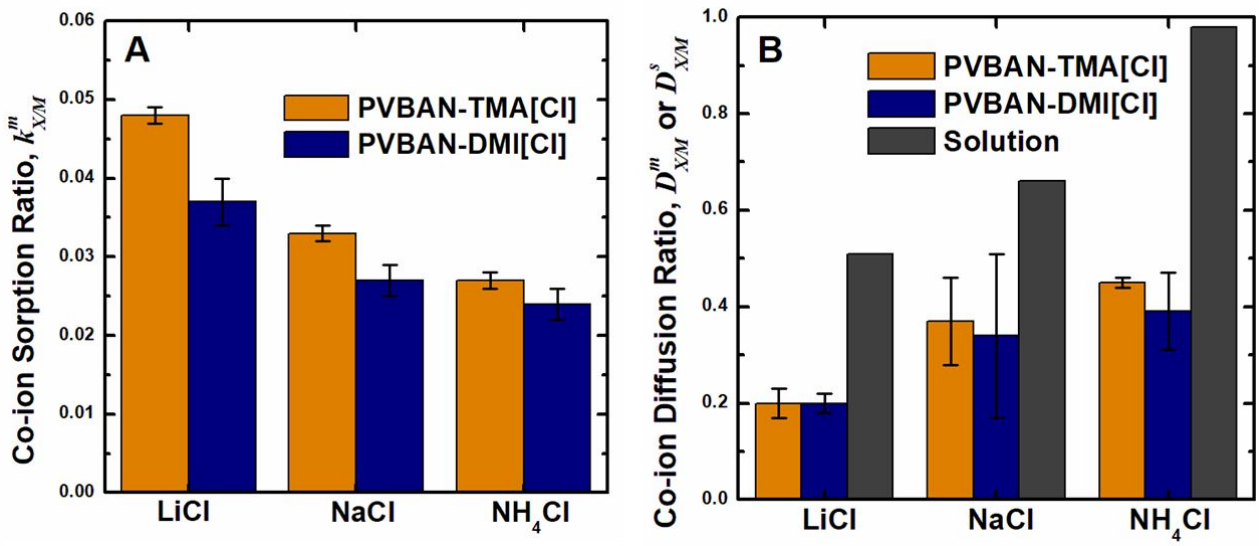

Figure 4. The (A) $k^m_{X/M}$ and (B) $D^m_{X/M}$ and $D^s_{X/M}$ values of the two AEMs in 0.5mol/L aqueous electrolyte solutions of lithium chloride, sodium chloride and ammonium chloride, i.e., electrolytes with different co-ions. The $k^m_{X/M}$, $D^m_{X/M}$ and $D^s_{X/M}$ values were calculated from measured k^m_s , c^m_A , D^m_s and σ^m_s values, and the standard deviation values were calculated from the standard deviation of k^m_s , c^m_A , D^m_s and σ^m_s via error propagation.

$$D_{X/M}^m = \frac{D_X^m}{D_M^m} \quad (17)$$

$$D_s^m = \frac{D_X^m D_M^m \left(c_X^m + c_M^m\right)}{c_X^m D_X^m + c_M^m D_M^m} \quad (18)$$

$$\sigma_s^m = \frac{F^2}{RT}\left(c_M^m D_M^m + c_X^m D_X^m\right) \quad (19)$$

where c_s^s is the concentration of the external solution, k_s^m is the salt sorption coefficient, which defines sorption of salt from the external solution into the membrane, c_s^m is the salt concentration in the membrane, D_s^m is the salt diffusivity in the membrane, σ_s^m is the membrane ionic conductivity, F is Faraday's constant, R is the gas constant and T is the absolute temperature.

The measured k_s^m, c_A^m, D_s^m and σ_s^m values are reported in Section S7 of the Supporting Information. Co-ion and counter-ion transport was analysed using the calculated $k_{X/M}^m$, $D_{X/M}^m$ and $D_{X/M}^s$ values. The subsequent discussion compares the $k_{X/M}^m$, $D_{X/M}^m$ and $D_{X/M}^s$ values between the two AEMs and among the different ions to provide insight into fixed charge group and/or ion specific transport properties.

3.3.1. Electrolytes with Different Co-ions

When the AEMs were characterized using electrolytes featuring different co-ions, i.e., lithium chloride, sodium chloride and ammonium chloride, the $k_{X/M}^m$ values of PVBAN-DMI[Cl] were found to be approximately 20% lower than that of PVBAN-TMA[Cl] (Figure 4A). This result likely stems from the larger deswelling degree and the higher c_A^m of PVBAN-DMI[Cl] in the 0.5mol/L electrolyte solutions. Ultimately, this phenomenon can be related back to the lower hydrophilicity of the DMI fixed charge group, and the result suggests that less hydrophilic fixed charge groups may enhance the overall co-ion exclusion performance of an AEM.

The $D_{X/M}^m$ values of the two AEMs were less influenced by the fixed charged group type. For all electrolytes, the $D_{X/M}^m$ values for PVBAN-DMI[Cl] are statistically indistinguishable from those values for

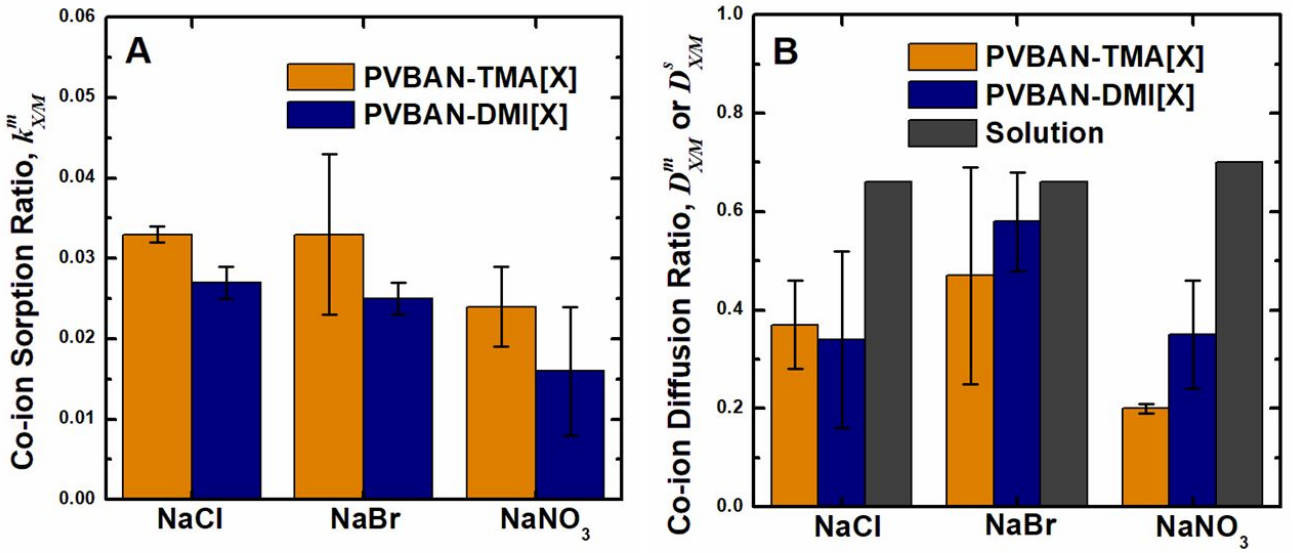

Figure 5. The (A) $k_{X/M}^m$ and (B) $D_{X/M}^m$ and $D_{X/M}^s$ values of the two AEMs in 0.5mol/L aqueous electrolyte solutions of sodium chloride, sodium bromide and sodium nitrate, i.e., electrolytes with different co-ions. The $k_{X/M}^m$, $D_{X/M}^m$ and $D_{X/M}^s$ values were calculated from measured k_s^m, c_A^m, D_s^m and σ_s^m values, and the standard deviations were calculated from the standard deviations of the k_s^m, c_A^m, D_s^m and σ_s^m properties via error propagation.

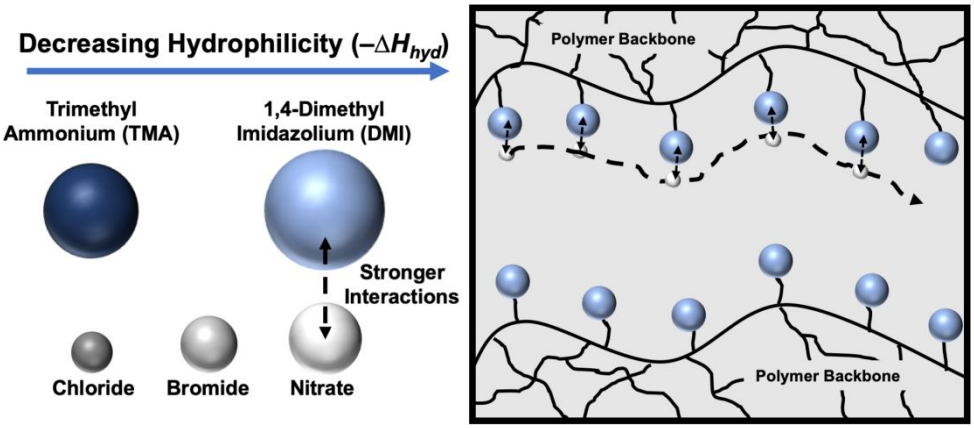

Figure 6. Schematic illustration of a proposed mechanism where stronger interactions between the fixed charge groups and counter-ions that have similar hydration properties may restrict counter-ion diffusion in the membrane.

PVBAN-TMA[Cl] (**Figure 4B**). This result suggests that the relative diffusion properties may be more significantly influenced by the nature of the electrolyte as opposed to the specific fixed charge group.

Overall, the change in $k_{X/M}^m$ upon switching between the TMA and DMI fixed charge group was about 20% for lithium chloride, sodium chloride and ammonium chloride. The change in $D_{X/M}^m$ upon switching between the TMA and DMI fixed charge group was essentially negligible. As such, co-ion sorption properties appear have the strongest influence on apparent permselectivity for these AEMs. The DMI fixed charge group resulted in lower water content and higher fixed charge group concentration compared to the TMA fixed charge group, and this situation favored co-ion exclusion in PVBAN-DMI[Cl], though the observed differences in co-ion exclusion between the two materials did not significantly affect the measured apparent permselectivity.

3.3.2. Electrolytes with Different Counter-ions

When the AEMs were characterized using electrolytes with different counter-ions, i.e., sodium chloride, sodium bromide and sodium nitrate, changing the fixed charge group from TMA to DMI did not have as uniform an influence on $k_{X/M}^m$ (Figure 5A) as was observed when the co-ion was changed (Figure 4A). When sodium chloride was used to characterize the membranes, the $k_{X/M}^m$ value for PVBAN-DMI[X] were lower than those of PVBAN-TMA[X]. When sodium bromide or nitrate were used to characterize the membranes, switching the fixed charge group had a less significant effect on the value of $k_{X/M}^m$ .This result also may be due to the larger deswelling degree and the resulting higher c_A^m of PVBAN-DMI[X] compared to PVBAN-TMA[X], but in general, switching the counter-ion had less of an effect on ion exclusion compared to switching the co-ion.

When the sodium chloride or sodium bromide electrolytes were used to characterize the materials, the PVBAN-DMI[X] $D_{X/M}^m$ values were statistically similar to those values for PVBAN-TMA[X]. When sodium nitrate was used to characterize the materials, however, the PVBAN-DMI[X] value was greater than that of PVBAN-TMA[X] (Figure 5B). This observation differs from the statistically equivalent $D_{X/M}^m$ values of PVBAN-DMI[Cl] and of PVBAN-TMA[Cl] when lithium chloride, sodium chloride and ammonium chloride were used (Figure 4B), and this result suggests that interactions between the counter-ion and the fixed charge group may be important for determining the diffusion properties of the material as discussed in more detail in the next section.

3.3.3. Reduction in Counter-ion Diffusion and Specific Binding

When the two AEMs were characterized using electrolytes with chloride and bromide counter-ions (i.e., lithium chloride, sodium chloride, ammonium chloride and sodium bromide), the $D_{X/M}^m$ values of PVBAN-DMI[X] were statistically equivalent to those of PVBAN-TMA[X]. However, when an electrolyte with a nitrate counter-ion (i.e., sodium nitrate) was used to characterize the membranes, the $D_{X/M}^m$ value of PVBAN-DMI[NO_3] was greater than that of PVBAN-TMA[NO_3]. Moreover, since PVBAN-DMI[NO_3] was less hydrophilic than PVBAN-TMA[NO_3], this observation contrasted the generally accepted view that less hydrophilic membranes typically restrict ion diffusion to a larger extent compared to more hydrophilic membranes.[17, 49] Counter-ion condensation or binding/pairing effects between the weakly hydrated ion and fixed charge group (i.e., nitrate and DMI, respectively) may explain this observed phenomena (Figure 6).

The basis for this explanation originates from the *Law of Matching Water Affinities* (LMWA) proposed by Collins.[56, 57] The LMWA asserts that cations and anions (or ions and ionic fixed charge groups) can form stable ion pairs if the enthalpy of hydration (considered to be a measure of water affinity) of the two ions are similar.[56, 57] A more straightforward explanation of this law is that more hydrophilic cations or ion-changed sites will tend to form stable pairs with more hydrophilic anions, and *vice versa*.

In this study, the enthalpy of hydration of DMI is less negative than that of TMA. Additionally, nitrate had the least negative enthalpy of hydration out of the anions considered in this study. Therefore, nitrate and the DMI fixed charge group would be most likely, of the systems considered in this work, to form ion pairs or undergo counter-ion condensation according to the LMWA. These interactions between DMI and nitrate could immobilize, at least to some extent, the nitrate counter-ions and reduce the counter-ion diffusivity (D_M^m). This reduction in D_M^m would ultimately lead to an increase in $D_{X/M}^m$ (Equation 15) for PVBAN-DMI[NO_3].

4. Conclusions

Two styrene- and acrylonitrile-based crosslinked AEMs with 1,4-dimethyl imidazolium and trimethyl ammonium fixed charge groups, respectively, were synthesized. The polymer backbones and IEC values were controlled to be essentially equivalent with the goal of making the only substantial difference between the two AEMs the fixed charge group type. The water uptake, apparent permselectivity, co-ion to counter-ion concentration and diffusivity ratios of the two AEMs were measured and analyzed to understand the effects of fixed charge group type on permselectivity and ion transport.

First, the apparent permselectivity was influenced by fixed charge group to a relatively small extent compared to the co-ion type, and the apparent permselectivity was influenced by counter-ion type to an even smaller extent. The observed differences in the apparent permselectivity properties appear to result primarily from differences in co-ion sorption properties. Second, the AEM with the less hydrophilic fixed charge group deswelled to a greater extent in aqueous electrolyte solutions compared to the AEM with the more hydrophilic fixed charge group. The resulting higher fixed charge group concentration of the less hydrophilic AEM made it more effective at excluding co-ions compared to the more hydrophilic AEM. Third, fixed charge groups may pair/bind more strongly with counter-ions that have similar hydrophilicity (i.e., similar enthalpy of hydration), and stronger pairing/binding could restrict counter-ion diffusion. For example, the diffusion of the less hydrophilic counter-ion (nitrate) was restricted to a larger extent in the less hydrophilic PVBAN-DMI material.

Ultimately, results from this study quantified the influence of fixed charge group type on the apparent permselectivity

properties of two AEMs. Though the influence of the fixed charge groups on apparent permselectivity was relatively small, it was demonstrated that the fixed charge group hydrophilicity is strongly coupled to membrane apparent permselectivity properties. Additionally, this study further illuminates ion specific transport properties of anion exchange membranes that are important for a wide range of electro-membrane processes.

5. Conflicts of Interest

There are no conflicts of interest to declare.

6. Acknowledgements

This material is based upon work supported in part by the National Science Foundation under Grant No. CBET-1752048.

Notes and References

1. F. Helferich, *Ion exchange*, McGraw-Hill Book Company, Inc., 1962.
2. J. Kamcev and B. D. Freeman, *Annu. Rev. Chem. Biomol. Eng.*, 2016, **7**, 111-133.
3. T. Sata, *Ion exchange membranes*, The Royal Society of Chemistry, 2004.
4. H. Strathmann, *Introduction to membrane science and Technology*, Wiley-VCH, 2011.
5. H. Strathmann, *Desalination*, 2010, **264**, 268-288.
6. Y.-J. Kim and J.-H. Choi, *Sep. Purif. Technol.*, 2010, **71**, 70-75.
7. B. E. Logan and M. Elimelech, *Nature*, 2012, **488**, 313.
8. X. Li, H. Zhang, Z. Mai, H. Zhang and I. Vankelecom, *Energy Environ. Sci.*, 2011, **4**, 1147-1160.
9. M. Ben Sik Ali, D. Jellouli Ennigrou and B. Hamrouni, *Environ. technol.*, 2013, **34**, 2521-2529.
10. J. R. Rao, B. Prasad, V. Narasimhan, T. Ramasami, P. Shah and A. Khan, *J. Membr. Sci.* , 1989, **46**, 215-224.
11. X. Deming, S. Dezheng and L. Xiaoying, *Desalination*, 1987, **62**, 251-257.
12. L. Marder, A. M. Bernardes and J. Z. Ferreira, *Sep. Purif. Technol.*, 2004, **37**, 247-255.
13. Z. Amor, B. Bariou, N. Mameri, M. Taky, S. Nicolas and A. Elmidaoui, *Desalination*, 2001, **133**, 215-223.
14. V. Roquebert, S. Booth, R. S. Cushing, G. Crozes and E. Hansen, *Desalination*, 2000, **131**, 285-291.
15. Y. Takeo, S. Manabu, T. Tatuo and K. Ichiro, *Bull. Chem. Soc. Jpn.*, 1960, **33**, 1740-1740.
16. T. Luo, S. Abdu and M. Wessling, *J. Membr. Sci.*, 2018, **555**, 429-454.
17. G. M. Geise, D. R. Paul and B. D. Freeman, *Prog. Polym. Sci.*, 2014, **39**, 1-42.
18. T. Sata, *J. Membr. Sci.*, 1994, **93**, 117-135.
19. P. Sivaraman, J. G. Chavan, A. P. Thakur, V. R. Hande and A. B. Samui, *Electrochim. Acta*, 2007, **52**, 5046-5052.
20. M. Vaselbehagh, H. Karkhanechi, R. Takagi and H. Matsuyama, *J. Membr. Sci.*, 2015, **490**, 301-310.
21. H. Farrokhzad, M. R. Moghbeli, T. Van Gerven and B. Van der Bruggen, *React. Funct. Polym.*, 2015, **86**, 161-167.
22. E. Güler, W. van Baak, M. Saakes and K. Nijmeijer, *J. Membr. Sci.*, 2014, **455**, 254-270.
23. S. Abdu, M.-C. Martí-Calatayud, J. E. Wong, M. García-Gabaldón and M. Wessling, *ACS Appl. Mater. Interfaces*, 2014, **6**, 1843-1854.
24. M. L. Bruening and D. M. Sullivan, *Chem. Eur. J.* , 2002, **8**, 3832-3837.
25. C. Cheng, A. Yaroshchuk and M. L. Bruening, *Langmuir*, 2013, **29**, 1885-1892.
26. H. Luo, J. Aboki, Y. Ji, R. Guo and G. M. Geise, *ACS Appl. Mater. Interfaces*, 2018, **10**, 4102-4112.
27. R. Nagarale, G. Gohil, V. K. Shahi and R. Rangarajan, *Colloid Surf. A Physicochm. Eng. Asp.*, 2004, **251**, 133-140.
28. T. Sata, T. Sata and W. Yang, *J. Membr. Sci.*, 2002, **206**, 31-60.
29. B. Qiu, B. Lin, L. Qiu and F. Yan, *J. Mater. Chem.* , 2012, **22**, 1040-1045.
30. H. Luo, K. Chang, K. Bahati and G. M. Geise, *Environ. Sci. Technol. Lett*, 2019, **6**, 462-466.
31. H. Luo, K. Chang, K. Bahati and G. M. Geise, *J. Membr. Sci.*, 2019, **590**, 117295.
32. H. Ju, A. C. Sagle, B. D. Freeman, J. I. Mardel and A. J. Hill, *J. Membr. Sci.*, 2010, **358**, 131-141.
33. J. Kamcev, E.-S. Jang, N. Yan, D. R. Paul and B. D. Freeman, *J. Membr. Sci.*, 2015, **479**, 55-66.
34. Y. H. Zhao, M. H. Abraham and A. M. Zissimos, *J. Org.*, 2003, **68**, 7368-7373.
35. J. E. K. Huheey, Ellen A.; Keiter, Richard L., *Inorganic chemistry: principles of structure and reactivity*, New York, NY: Harper Collins College Publishers, 1993.
36. D. W. Smith, *J. Chem. Educ.*, 1977, **54**, 540.
37. C. E. Housecroft and H. D. B. Jenkins, *RSC Adv.*, 2017, **7**, 27881-27894.
38. R. Epsztein, E. Shaulsky, M. Qin and M. Elimelech, *J. Membr. Sci.*, 2019, **580**, 316-326.
39. D. L. Lide, *Handbook of chemistry and physics*, CRC Press, 2003 - 2004.
40. W. Xie, J. Cook, H. B. Park, B. D. Freeman, C. H. Lee and J. E. McGrath, *Polymer*, 2011, **52**, 2032-2043.
41. P. C. Wankat, *Separation process engineering*, Pearson Education, 2006.
42. Y. Ji and G. M. Geise, *Ind. Eng. Chem. Res.*, 2017, **56**, 7559-7566.
43. Y. Ji, H. Luo and G. M. Geise, *J. Membr. Sci.*, 2018, **563**, 492-504.
44. Y. Marcus, *Ion properties*, CRC Press, 1997.
45. K. S. Pitzer and G. Mayorga, *J. Phys. Chem.*, 1973, **77**, 2300-2308.
46. R. S. Kingsbury, S. Flotron, S. Zhu, D. F. Call and O. Coronell, *Environ. Sci. Technol.*, 2018, **52**, 4929-4936.
47. J. Crank, *The mathematics of diffusion*, Oxford university press, 1979.
48. R. W. Barker, *Membrane technology and appliations*, John Wiley & Sons, Ltd, 2004.
49. H. Zhang and G. M. Geise, *J. Membr. Sci.*, 2016, **520**, 790-800.
50. E. Axpe, D. Chan, G. S. Offeddu, Y. Chang, D. Merida, H. L. Hernandez and E. A. Appel, *Macromolecules*, 2019, **52**, 6889-6897.

51. G. M. Geise, H. S. Lee, D. J. Miller, B. D. Freeman, J. E. McGrath and D. R. Paul, *J. Polym. Sci. Pol. Phys.*, 2010, **48**, 1685-1718.
52. G. M. Geise, M. A. Hickner and B. E. Logan, *ACS Macro Letters*, 2013, **2**, 814-817.
53. C. Nam, T. J. Zimudzi, G. M. Geise and M. A. Hickner, *ACS Applied Materials & Interfaces*, 2016, **8**, 14263-14270.
54. G. M. Geise, H. J. Cassady, D. R. Paul, B. E. Logan and M. A. Hickner, *Phys. Chem. Chem. Phys.*, 2014, **16**, 21673-21681.
55. J. Kamcev, R. Sujanani, E.-S. Jang, N. Yan, N. Moe, D. R. Paul and B. D. Freeman, *J. Membr. Sci.*, 2018, **547**, 123-133.
56. A. Salis and B. W. Ninham, *Chem. Soc. Rev.*, 2014, **43**, 7358-7377.
57. K. D. Collins, *Biophys. J.* , 1997, **72**, 65-76.